THE FRONTIERS COLLECTION

Boris Murmann
Bernd Hoefflinger (Eds.)

NANO-CHIPS 2030

On-Chip AI for an Efficient Data-Driven World

Springer

In Murmann & Hoefflinger (2020) NANO-CHIPS 2030
On-Chip AI for an Efficient Data-Driven World, Springer

Chapter 24
Artificial Retina: A Future Cellular-Resolution Brain-Machine Interface

Dante G. Muratore and E. J. Chichilnisky

24.1 Brain-Machine Interfaces of the Future

A *brain-machine interface* (BMI) is a device capable of providing a direct communication path between the nervous system and an external device. BMIs can be used in research to better understand the brain, and are increasingly intended for clinical applications, including treating hearing and vision loss, paralysis, and other consequences of degeneration and injury [1, 2]. In the future, BMIs will likely be used to augment human capabilities, including sensory acuity, control of complex devices, memory, attention and more. However, to realize this futuristic promise requires major advances in the design of circuits and systems for interfacing to the brain.

A BMI usually consists of a neural interface capable of sensing and/or eliciting neural activity, and a computing device that controls its operation. The neural interface can operate in any of several modalities—e.g. optical, electrical, magnetic—each with advantages and disadvantages [3]. In this chapter, we will focus on electrical neural interfaces; typically, arrays of electrodes for stimulating and recording neural activity. Thus, the performance of the interface is determined by the channel count and density, the signal-to-noise ratio (SNR) of recording and stimulation, and the bandwidth of wireless transmission of data to and from the device. However, the specifications for a neural interface that attempts to approach or exceed the capability of the neural circuitry can pose major challenges in terms of size and power consumption for an implanted device.

D. G. Muratore (✉)
Department of Electrical Engineering, Stanford University, Stanford, CA 94305, USA
e-mail: dantegmuratore@gmail.com

Wu Tsai Neurosciences Institute, Stanford University, Stanford, CA 94305, USA

E. J. Chichilnisky
Department of Neurosurgery, Stanford University, Stanford, CA 94305, USA
e-mail: ej@stanford.edu

Department of Ophthalmology, Stanford University, Stanford, CA 94305, USA

© Springer Nature Switzerland AG 2020

B. Murmann and B. Hoefflinger (eds.), *NANO-CHIPS 2030*,
The Frontiers Collection, https://doi.org/10.1007/978-3-030-18338-7_24

What exactly are the specifications for an effective neural interface? Ideally, one would like to independently access each neuron in a region of the nervous system. Obviously, this is often not feasible: systems that communicate with many neurons usually do not achieve single-cell resolution, while high-resolution systems can only record from a limited number of neurons. The optimal trade-off of resolution and scale may depend on the specific application; thus, the design of future BMIs should be guided by a deep understanding of how information is encoded in the targeted part of the nervous system.

For example, accumulating evidence in intracortical motor BMIs shows that, for current devices, *spike sorting* (distinguishing electrical impulses, or spikes, recorded from different neurons) does not produce a substantial increase in decoding performance [4–8]. Instead, if only threshold detection is performed on the recorded data, the specifications on the neural interface can be relaxed and the power consumption per channel can be drastically decreased, allowing more channels to be implanted [9]. However, as a better understanding of the neural circuitry in the motor cortex develops and recording devices with greater capabilities become available, systems that are capable of resolving individual cells could be valuable.

This evolution of design tradeoffs is already evident in the retina, likely because its function is better understood than other parts of the nervous system. Decades of research on the retina and visual system indicate that an effective interface that can replace retinal function lost to disease should reproduce the natural pattern of activation of the cells that transmit visual signals to the brain [10]. Because diverse cell types are intermixed in the retinal circuitry, such a device will need to sort spikes coming from different cells and sort the recorded cells into different cell types. This in turn will permit the device to stimulate each cell and cell type in a way that matches natural function. No BMI has ever been developed that can achieve these goals; however, advances in circuit design as well as in our understanding of the retina now bring this goal within reach.

In this chapter, we describe how the retina transduces light into a neural code that then is processed by the brain, and why this architecture implies that a high-fidelity retinal implant should operate at cellular and cell-type resolution. We then discuss the limited performance of first-generation retinal prostheses, which were not designed with this goal in mind. Finally, we describe a project at Stanford University aimed at developing an *artificial retina* that takes into consideration cell-type specificity of retinal signals and aims to reproduce the neural code at its natural resolution. Finally, we comment briefly on the possible implications for future BMIs.

24.2 Neuroscience of the Retina and Vision

The retina is a multi-layer structure at the rear of the eye containing neural circuitry that transduces the visual image into electrical signals, processes those signals, then transmits the results to the brain so that a visual image of the external world can be

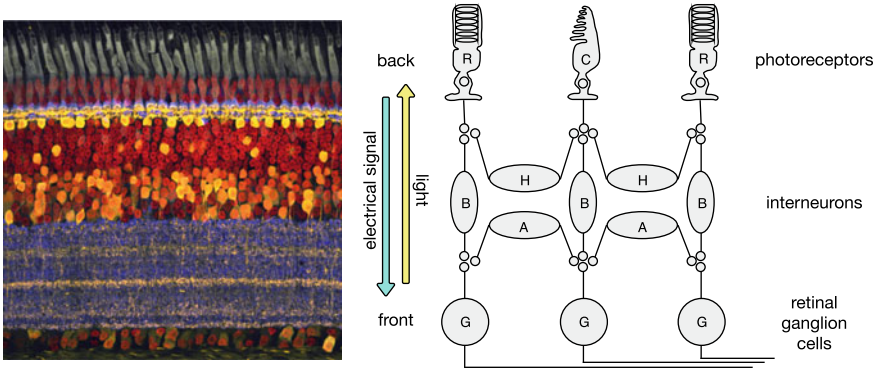

Fig. 24.1 Left: retina cross-section (from [12], © Abrams 2010). Right: schematic of retina layers and cell classes: (R)od and (C)one photoreceptors; (H)orizontal, (B)ipolar, and (A)macrine interneurons; (G)anglion cells

formed [11]. A cross-section of the retina highlights three different layers: *photoreceptors*, *interneurons*, and *retinal ganglion cells* (RGCs) (Fig. 24.1). The incoming light passes through the retina, which is mostly transparent, and arrives at the photoreceptors, where it is transduced into electrical signals. The signals coming from photoreceptors are integrated by interneurons, which in turn synapse onto RGCs, the output cells of the retina. As with most neurons, RGCs consist of a cell body (or *soma*), and a long nerve fiber (or *axon*) that transmits its all-or-none electrical impulses (or *spikes*) to target neurons in the brain. The axons of RGCs form the optic nerve, which routes visual information to many different parts of the brain for subsequent processing. Vision is the result of this fascinating distributed biological system.

The retina has several gross structural features that are important for neural interface design. In an *en face* view of the primate retina (Fig. 24.2; [13]) bundles of axons are visible, traveling from RGCs towards the optic nerve. Interestingly, axon bundles avoid passing through an area in the central retina called the *fovea*, presumably to

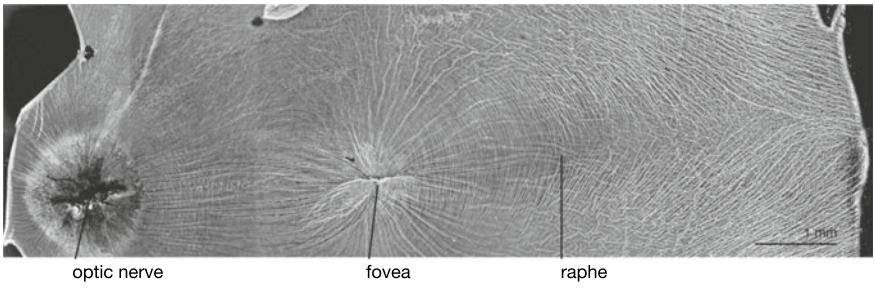

Fig. 24.2 Photograph of a flattened macaque retina, with landmarks and locations relevant for epiretinal implants shown (from [13], © APS 2017)

preserve optical clarity in this high-resolution region at the center of the visual field. In the center of the fovea, interneurons and RGCs are displaced laterally, providing a direct light path to the photoreceptors. As a result, the RGC layer is several cells thick, as opposed to the rest of the retina, where RGCs form a single layer. The high-resolution fovea occupies a small part of the retina, while the remainder of the visual scene is captured at low resolution by the peripheral retina. In fact, at approximately 15° outside the fovea, the visual acuity of a healthy person is equal to that of a legally blind patient.

The reason we can look at the Colosseum in Rome or the Golden Gate Bridge in San Francisco and reconstruct a high-resolution image, in spite of the small size of the fovea, is that our eyes constantly explore the scene in a series of active fixations connected by rapid eye movements. The eye focuses the fovea on certain features of the visual image, and moves quickly between them (Fig. 24.3; [14]). These different views are then integrated by the brain to produce a coherent representation of the visual scene.

Certain kinds of vision loss, such as macular degeneration and retinitis pigmentosa, arise from the loss of photoreceptors which normally transduce light. However, many other neurons, notably the RGCs, remain in large numbers. Therefore, a potential way to treat this kind of blindness is a device that uses an implanted neural interface to electrically stimulate RGCs (Fig. 24.4), causing them to fire spikes that are transmitted to the brain. In addition to a neural interface, such a device requires a camera to capture the image, and a processing unit to determine the appropriate patterns of electrical stimulation. First-generation devices with this general design have been shown to produce visual perception in profoundly blind patients, though performance has been limited (see Sect. 24.4).

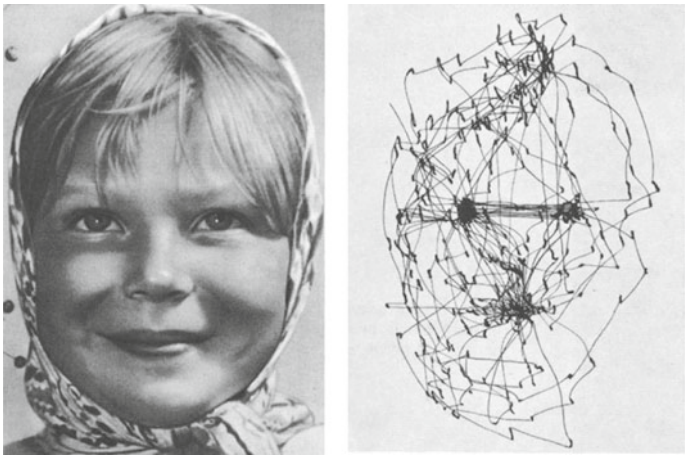

Fig. 24.3 Pattern of eye movements over an image during 3 minutes of free viewing by a human subject (from [14], © Springer 1967)

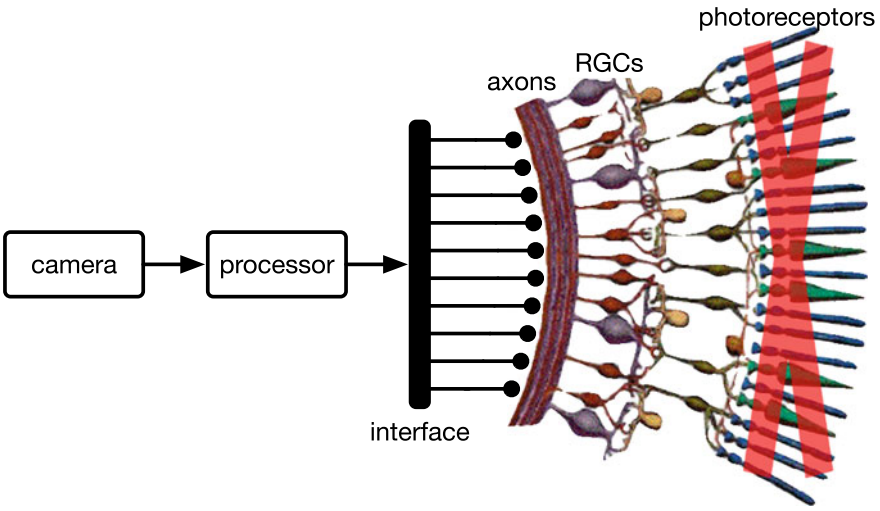

Fig. 24.4 Schematic of retina with degenerated photoreceptors, and epi-retinal prosthesis. The prosthesis consists of a camera, a processing unit, and a neural interface to electrically stimulate RGCs

A major obstacle to restoring high-fidelity vision with such devices, and arguably a key reason for the limited performance of first generation devices, is that there are many types of RGCs in the retina that deliver distinct visual signals to different targets in the brain (see [15–18]). For example, simultaneous activation of so-called ON and OFF type cells at a given location sends conflicting "messages" to the brain, indicating both a light increase, and a light decrease, at the same retinal location at the same time. Present-day retinal prostheses make no attempt to distinguish distinct cells or cell types, and therefore produce a non-specific, and thus profoundly scrambled, retinal signal of exactly this kind (see Sect. 24.4). These considerations suggest that to re-create the naturalistic neural code, and to produce high-fidelity artificial vision, requires that the distinct cell types be addressed independently. Because the different cell types are intermixed in the neural circuitry of the retina, this requires cellular resolution interfaces, with high channel count to recreate complex patterns in the neural network. Neural interfaces that operate this way—at the natural resolution of the neural circuitry—do not currently exist.

Note that, in principle, highly plastic neural circuits in the brain could adjust over time to accommodate scrambled retinal signals. Although a thorough treatment of visual plasticity and learning is out of the scope of this chapter, two major considerations argue against a major role for plasticity in artificial vision. First, plasticity is costly and complex to implement and regulate in any circuit, be it neural or electronic, and it is unlikely that evolutionary pressures would favor a visual brain with the ability to adjust itself to the highly non-biological stimulation provided by current prostheses. Second, a substantial rewiring of the distinct projections of different RGC types into the brain after prosthesis implantation is highly unlikely in adults,

and existing studies suggest that visual perception with prostheses changes little with experience [19].

Assuming that a retinal implant must reproduce the neural code at cellular and cell-type resolution in order to provide high-fidelity artificial vision, what are the specific scientific and engineering requirements? From an engineering point of view, we require the ability to control the spiking activity of each cell and cell type independently. From a scientific point of view, we must understand the natural pattern of activation of RGCs for a given image in order to reproduce it faithfully. Several decades of basic neuroscience research have accumulated a great deal of knowledge about the pattern of activation of RGCs; indeed, the retina is one of the best understood parts of the nervous system. Thus, at the moment, the limiting factor is engineering a device capable of cellular and cell type resolution over a large area of the retina.

24.3 Neurophysiology and Electrical Stimulation of Neurons

To understand how such a device might work and the state of the art, we will describe extracellular recording and stimulation of neural activity. Information in most neurons (including RGCs) is encoded in spikes, which are brief electrical impulses, i.e. perturbations in the voltage across the cell membrane. Because spikes are stereotyped all-or-none signals, information is conveyed only by the temporal pattern of spikes, not by the spike shape.

Understanding how spikes are generated in the cell sets the context for thinking about how electrical recording and stimulation can be used to monitor and control neural activity. The cell's membrane potential is controlled by a wide variety of *ion channels*, proteins that control the flow of ions [predominantly sodium (Na+) and potassium (K+)] across the cell membrane by opening and closing in response to voltage changes and binding of neurotransmitters [20]. Under resting conditions, the cell potential is ≈ -70 mV with respect to the extracellular medium, due to the different ionic concentrations inside and outside of the cell that are maintained by cellular pumps. If a signal from another neuron, or an external stimulus, depolarizes the cell above a certain threshold level (≈ -50 mV), then positive feedback from voltage-gated channels will cause the neuron to generate a spike—a stereotyped depolarization to about $+30$ mV that lasts about 1 ms. During the spike, the Na+ permeability initially increases rapidly, bringing in positive charge and further increasing the membrane potential (positive feedback). Then, the slower K+ channels are activated, allowing positive charges to flow out of the cell, and returning the intracellular potential to its resting state (negative feedback). Note that because ion channels open in response to voltage changes, spikes can be generated artificially by applying electric fields outside the cell. Furthermore, because these ionic currents are large, the polarization during a spike can be monitored outside the cell by recording

the extracellular potential using a microelectrode. The dispersive medium between the cell and the microelectrode introduces a signal attenuation, so that, typical extracellularly recorded spikes are ≈100 μV in amplitude, as opposed to the ≈100 mV change in the membrane potential.

Thus, neurons are de facto electrical processing units: they signal information with electrical impulses, and these impulses can be recorded and elicited by an electrical device outside the cell. Hence, the electrical domain is a natural one for the development of neural interfaces.

The way neurons produce spikes is crucial for identifying the origin of spikes recorded extracellularly (*spike sorting*; [21–23]) and for achieving single-cell resolution. The extracellularly-recorded spike waveform for any given cell is consistent over time and reflects the distribution of ion channels on the cell and spatial relationship between the cell and the recording electrode. Thus, if an electrode records spikes from two cells, their waveforms will typically be different, making it possible to distinguish the signals from the two cells. If an array of electrodes is used, the same cell can be recorded on multiple electrodes, increasing the spatial information for spike sorting.

The way neurons produce spikes can also inform the design of electrical stimulation for neural interfaces. An electrical model of RGCs can be used to simulate the membrane potential as a response to an external stimulus [24]. This simulation can inform the specifications on the stimulation pulse (i.e. duration and amplitude)—for example, results in [25] present numerical and analytical models of strength-duration curves for eliciting a spike.

In summary, interfacing with the nervous system in the electrical domain is a natural choice, given that neurons communicate with electrical signals. In particular, neurons encode information in spikes, which are comparatively easy to record and elicit without manipulating the internals of the cell.

24.4 First-Generation Epiretinal Prostheses

The first generation of retinal prostheses used electrical stimulation to elicit neural activity and artificial vision in blind human patients [10]. This technology development produced striking advances and an exciting proof of concept, but also fell short of the goal of restoring high-quality vision. Here, we focus on epiretinal devices, which are implanted on the surface of the retina to directly stimulate RGCs (see [10, 26–30] for a more complete review). The Argus devices developed by Second Sight constituted the first and largest commercial effort. Argus I was a first-generation prototype approved for a clinical trial aimed at establishing safety. Positive results of this trial on 6 patients motivated the development of Argus II, the only epiretinal device approved (in 2013) by the U.S. Food and Drug Administration (FDA) for clinical use. Argus II was initially implanted on 30 patients between 2007 and 2009, and in more than 150 additional patients since FDA approval [31]. However, in 2019, Second Sight stopped selling the device.

First-generation epiretinal prostheses provided a wealth of useful information. Most notably, stimulation of RGCs in profoundly blind patients with retinal degeneration elicits artificial visual perception (*phosphenes*). Phosphenes have been described by patients as being large, elongated and irregular [32, 33]. Their brightness and size were modulated with variations in the stimulation parameters (amplitude and frequency) [34]. Stimulation thresholds for light perception were well below the safety limits for electroporation [35, 36] and charge injection for most common electrode materials [37–39]. Notably, stimulation thresholds were highly dependent on the distance between the implant and the retinal surface, making obvious the need for keeping the array in close proximity to the retina [40].

However, the current state of the art of epiretinal prostheses, including the Argus II, can be summed up as such: no blind patient would trade their cane or guide dog for one. The artificial vision achieved with these devices is coarse, irregular, and difficult to relate to the objects in the visual scene [10]. A feature of first-generation devices that may play a role in their limited function is the small number of channels (e.g., 60 electrodes in Argus II), which is arguably insufficient to recreate a high-resolution image. One way to gain intuition about the required number of channels is to examine an image rendered with different numbers of pixels (Fig. 24.5; [41]). In the example reported below, the content of the image becomes clear when using a few thousand pixels. Because retinal neurons are not mere pixel detectors, the number of channels in a retinal implant and the effective number of pixels in perception are not directly comparable quantities. However, it seems clear that high-resolution visual restoration will require more independent stimulating channels.

Another issue with existing epiretinal devices is that they simultaneously activate many ganglion cell types due to the size of the stimulating electrodes (typically 50–500 μm in diameter). As discussed above, different cell types encode very different types of information, and failing to respect this specificity will likely lead to poor visual restoration. Increasing the spatial resolution of electrodes will also help with another problem faced by epiretinal devices: activation of unwanted axon bundles, which reside between the target ganglion cells and the microelectrode array and carry spikes from distant RGCs to the brain (Fig. 24.6). Activating axon bundles is almost

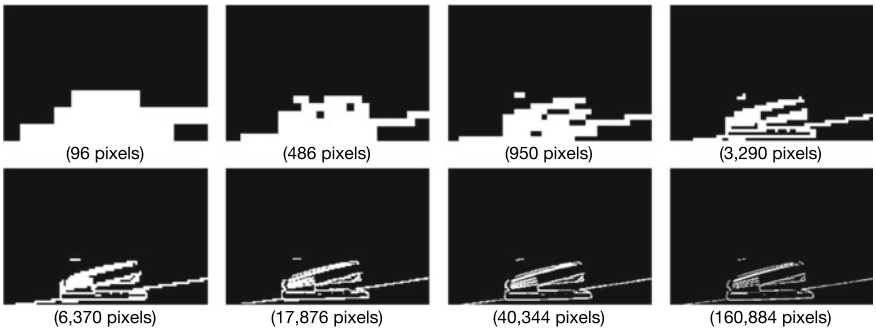

Fig. 24.5 Image of a stapler rendered with different numbers of pixels (from [41], © Elsevier 2015)

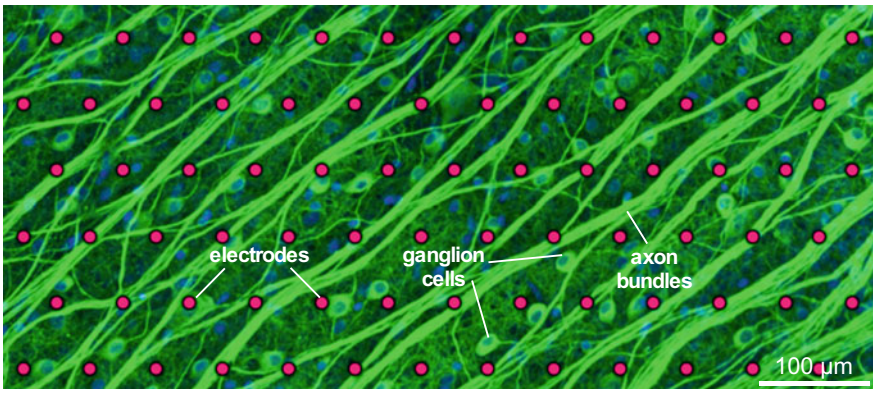

Fig. 24.6 Primate retinal ganglion cells, axon bundles, and overlying electrode array [13]

certain to degrade the image, because the originating cells and thus the location and nature of the visual signal they convey are varied and unknown. High-density arrays of small electrodes can increase the probability of being able to stimulate neurons without also activating axon bundles [13].

Axon activation can also be avoided by *subretinal* prostheses, which activate retinal interneurons rather than RGCs ([42, 43]; see [10]). These devices can be relatively simple and modular and show greater promise for vision restoration in the near future. However, the technical advantages of axon avoidance and interfacing to neurons at an earlier level of retinal processing are accompanied by severe limitations: limited scientific information about the neural code of the interneuron cell types, and the inability to record and precisely control their activity—both limitations arising because retinal interneurons are among the few cell groups in the central nervous system that signal with graded voltages rather than spikes. Hence, subretinal implants have little promise for accurately reproducing the neural code of the retina with cellular and cell-type resolution, and no path for extension to brain interfaces, and will not be discussed further.

In summary, first-generation prostheses demonstrate the possibility of vision restoration, but lack the ability to stimulate many cells with cellular and cell-type resolution. As a result, the neural code that is transmitted to the brain is severely distorted, limiting sight restoration.

24.5 The Stanford Artificial Retina

To improve on the state of the art, we propose a novel architecture for retinal implants—an *artificial retina* designed to adapt itself to the particular cells and cell types in the host circuitry, in order to faithfully reproduce the naturalistic neural code. Specifically, the device will have larger and denser electrode arrays to interface with

many cells at their native spatial resolution, and the ability to record spikes in order to calibrate the device to the underlying biological circuit. We make a distinction between retinal prostheses of the past, and artificial retinas of the future, to highlight that the goal of an artificial retina is to actually replace the natural function of the neural circuitry of the retina.

Our approach is based on an extensive set of neurophysiological experiments in isolated retina, which serve as a laboratory prototype for a future clinical device. This work builds on a long history of experiments using various technologies and animal models; here, we focus specifically on high-density large-scale electrical recording and stimulation in the monkey retina, the most relevant animal model for human vision. The results reveal that it is possible to reproduce the natural retinal signal with high fidelity [13, 44–46]. In the experiments, electrical activity in the peripheral macaque retina is recorded on a 512-electrode array with 30–60 μm pitch, and spike sorting is performed to identify distinct RGCs [47, 48]. To distinguish different cell types, the spatial and temporal light response properties of each cell are measured by correlating the images focused on the retina with the spiking activity of the cell, yielding functionally distinct clusters of cells [47, 48]. The accuracy of this cell type classification is confirmed by the fact that the spatial sensitivity profiles, or receptive fields, of each cell type form a mosaic covering the region of retina recorded [48–50] (Fig. 24.7). Electrical stimulation is then calibrated by passing varying amounts of current through each electrode on the array, while recording the elicited activity, exploiting the fact that the spike waveforms of different cells have already been learned during recording [13, 44–46]. Finally, electrical stimulation is tailored to the recorded cells and cell types in a manner that most accurately reproduces the natural

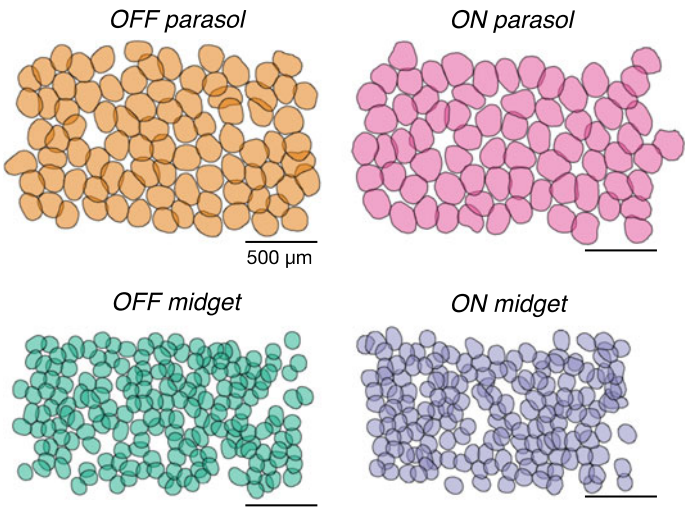

Fig. 24.7 Mosaics of receptive fields of the four major primate RGC types, obtained in a single multi-electrode recording from an isolated retina. The different RGC types overlap, but here, have been displaced for visibility (adapted from [53], © Cell Press 2019)

retinal activity (Fig. 24.8; [13, 44]). Spatial patterns of electrical stimulation through multiple electrodes simultaneously can also be used to fine-tune the activation of RGCs [51, 52].

The experimental approach described above informs the design of the future clinical device, and serves as a rapid prototyping platform for circuit-algorithm co-design and optimization. The proposed device [54] will operate bi-directionally, in three modes: *cell calibration* (recording only), *dictionary calibration* (stimulating and recording), and *runtime* (stimulating only) (Fig. 24.9). During cell calibration, the interface identifies the cells and cell types in close proximity to the electrode array, by recording spontaneous neural activity and sorting spikes from different RGCs. During dictionary calibration, the device determines how the different electrodes activate these cells, by recording and stimulating simultaneously. During runtime,

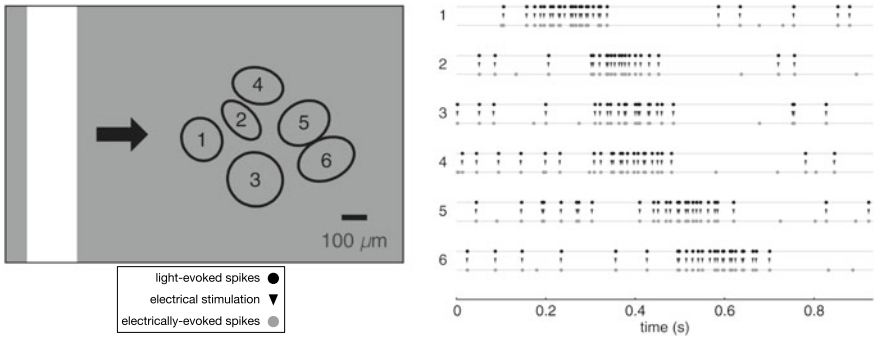

Fig. 24.8 Spatiotemporal visual and electrical activation of a local population of retinal ganglion cells. Left: A moving bar light stimulus is shown while recording from a population of six RGCs, with receptive fields indicated by ellipses, to determine the natural visual signal. Right: For each numbered cell, times are indicated for: spikes recorded during the moving bar light stimulus (black dots), applied current pulses during electrical stimulation (black triangles), and spikes evoked by electrical stimulation (grey dots). The alignment indicates that natural responses to light can be replicated by electrical stimulation with sub-millisecond temporal precision (from [44], © Cell Press 2014)

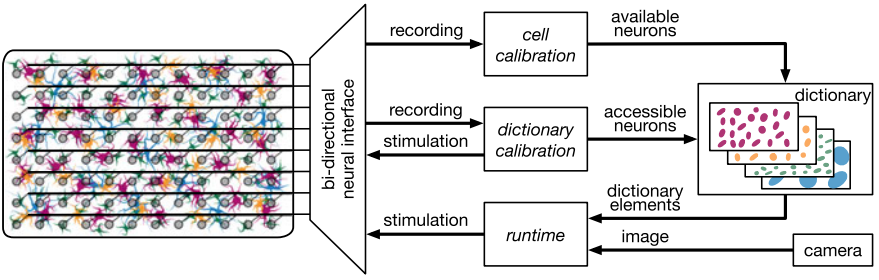

Fig. 24.9 System-level diagram of the proposed bi-directional neural interface with three operating modes

the interface stimulates the available cells to best approximate the correct neural signal based on the visual image captured by a camera. To produce meaningful visual signals (Fig. 24.5), the electrode array will have $>10^4$ channels, covering a relatively small part of the visual field, but one that is sufficient for useful vision. To interface at a resolution that roughly matches the neural circuitry, the electrode pitch will be ~30 μm or less. To faithfully encode a wide variety of visual images, the IC will have the ability to record and stimulate every channel independently.

24.5.1 Cell Calibration

Cell calibration (Fig. 24.10a) involves recording spontaneous activity to characterize the location and cell type of RGCs near the microelectrode array. Spikes generated by neurons are recorded by the interface and digitally processed to distinguish the spikes originating in different cells (*spike sorting*), requiring substantial computation to make sense of the large amount of data captured at the interface. We then leverage the fact that cell type classification can be performed solely based on electrical features of neurons [55]. A critical feature for this classification is the *electrical image* (EI) [47], which is the average spatiotemporal voltage waveform produced by the spike on the electrode array, a unique signature for each recorded cell (Fig. 24.11a). Another feature that helps distinguish different types of RGCs is the autocorrelation function of their spike trains (Fig. 24.11b). Typically, a neural network is trained to perform cell classification using these features (*classification*). Finally, the receptive field of each cell can be inferred from the EI, and its normal light response properties inferred from existing data.

Challenges: Although electrical features of RGCs can be very useful in classification, it is uncertain how completely classification can be accomplished, particularly given the variability between retinas, and the potential effect of retinal degeneration on the electrical properties of cells. Current work focuses on the use of very large data sets to improve classification. Also, to perform classification, the interface must record from many or all channels simultaneously in order to track the spatiotemporal evolution of spikes, resulting in data rates that are prohibitive in terms of energy and transmission bandwidth: e.g., 10,000 channels with 10-bit resolution at 20,000 samples per second generate 2 Gbps of recorded data. Without a radical change in the way neural interfaces are designed, the power dissipation during calibration will exceed the target for clinically viable devices by more than an order of magnitude. Fortunately, the signal of interest requires much less bandwidth, because a collection of neurons on the electrode array produce temporally and spatially sparse signals—thus, a continuous voltage recording on all channels is not needed. Such an observation about the statistics of neural spiking provides an opportunity to design a very efficient neural interface. This data explosion problem relates to most BMI applications and researchers have investigated a wide range of options to address it, such as on-chip spike sorting [56], on-chip compression [57–59], compressive sensing [60], and active analog multiplexing [61–63].

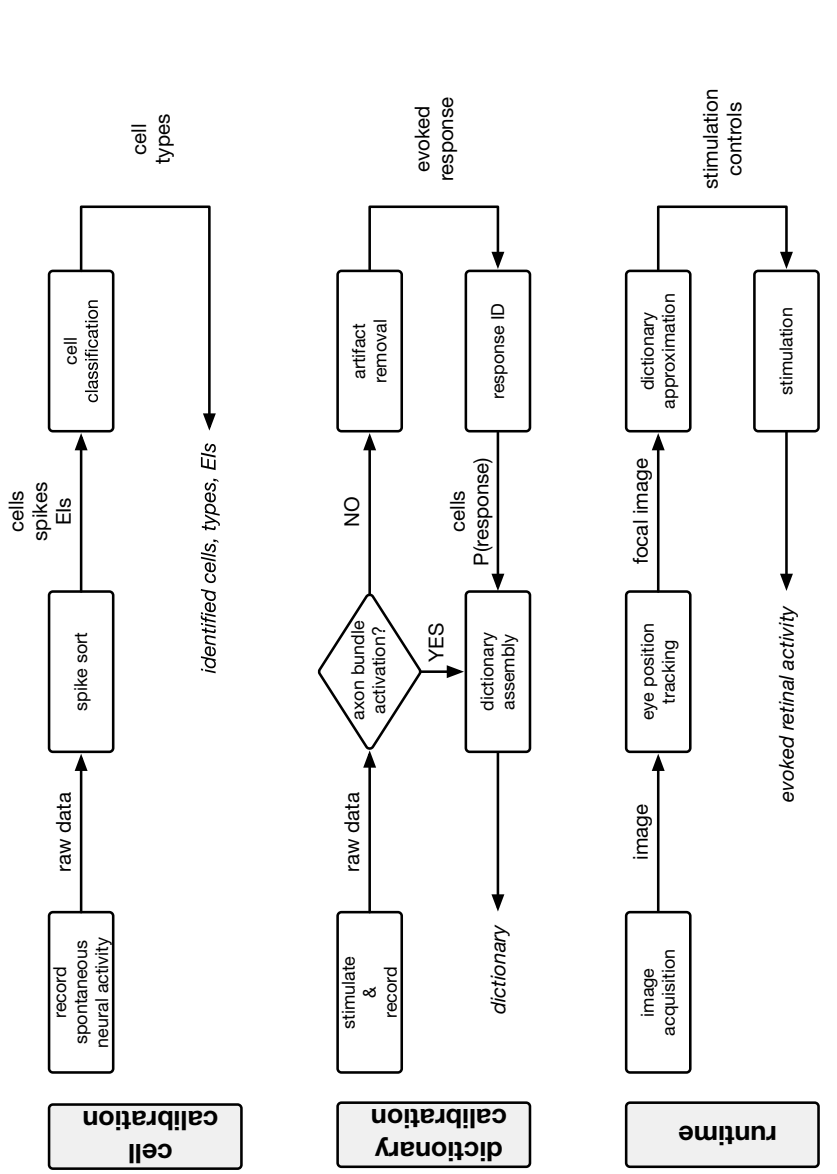

Fig. 24.10 Block diagram of each mode of operation for the proposed interface: **a** cell calibration, **b** dictionary calibration, and **c** runtime. Required components for each mode of operation are shown on the left

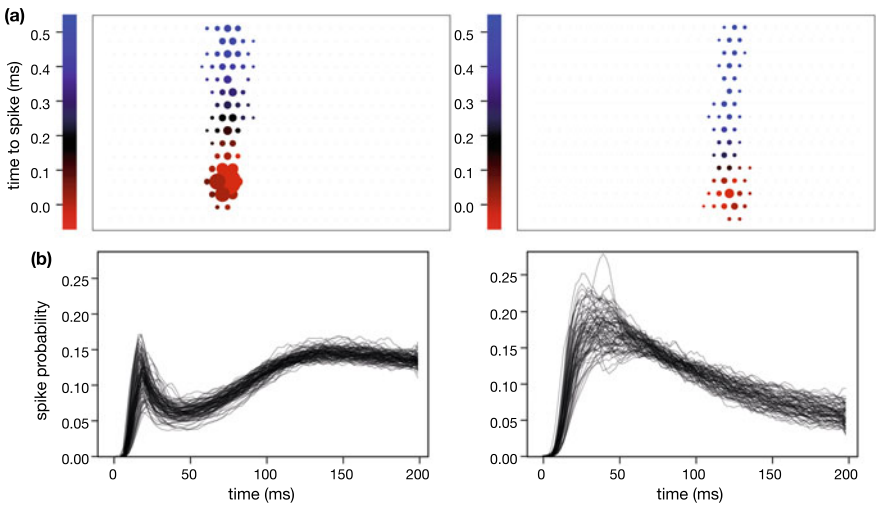

Fig. 24.11 Electrical features of neurons to be used for cell-type classification in blind retina. **a** Electrical image (EI) for an ON parasol and an ON midget cell from a primate retina. Each circle represents an electrode in the array, with radius indicating the average amplitude of the recorded spike, and color indicating its arrival time. Parasol EIs are usually larger and exhibit faster spike propagation than midget EIs. **b** Autocorrelation function of the spike train for a population of ON parasol cells and a population of OFF parasol cells in the primate retina

The electrical recording approach we propose performs lossy compression in the mixed-signal domain (i.e. before full digitization), exploiting two principles [64]. First, spikes are sparse in space and time, therefore we need only record spikes, and not voltage samples between spikes. Second, it is necessary only to identify and distinguish the spikes produced by different cells, therefore, spike waveforms need not be perfectly recorded. A scheme that exploits these facts is one in which the digitized voltage on a given electrode is retained only if it is different from the values on other electrodes. This can be accomplished efficiently with a *ramp analog-to-digital converter* (*ADC*) coupled with a *wired-OR readout* and a *unique-signal decoder*. During each sample, the ramp ADC indicates the input voltage with a brief pulse at a discrete time step proportional to the quantized voltage (the number of distinct time steps sets the ADC resolution and the ramp voltage range sets the ADC full-scale range). This is achieved by comparing the input signal to a ramp voltage that steps through the entire input range (Fig. 24.12a). The time of the pulse is captured using a counter that keeps track of the ramp steps. This is an efficient algorithm for digitizing many channels in an array because the ramp and the counter can be shared between all channels. Then, instead of reading the output pulses from each channel individually, channels are combined with an OR logic, across the rows and across the columns (Fig. 24.12b), to achieve the desired compression. Consequently, if only a single channel produces a pulse at a given time step (i.e., it is the only channel with a quantized voltage corresponding to the time step), then the channel location

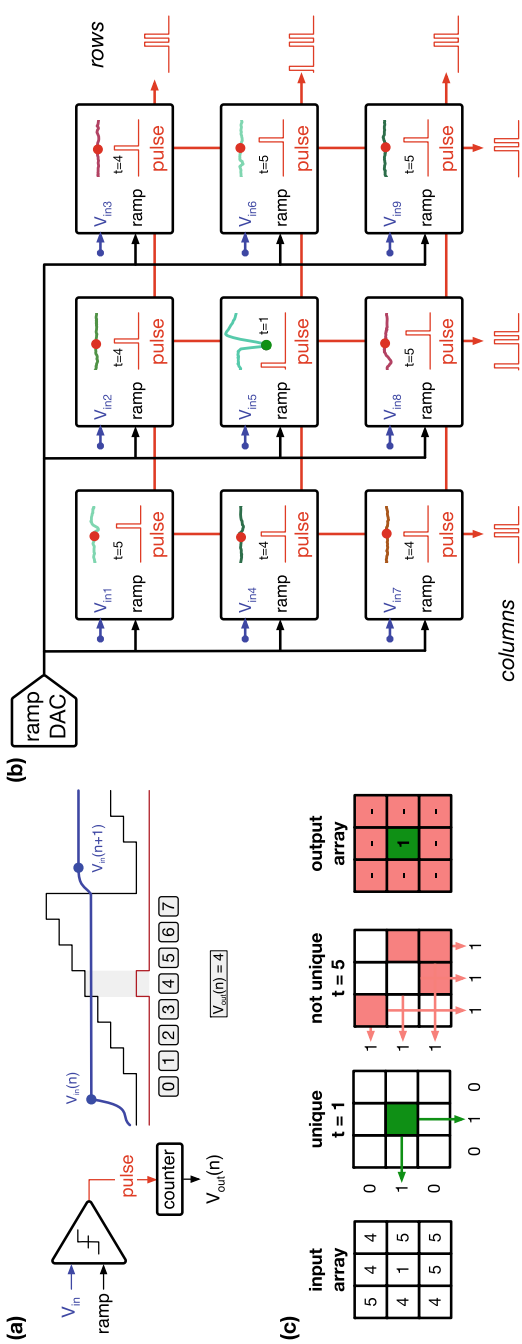

Fig. 24.12 Compressive readout strategy. **a** *Ramp ADC*: schematic and operation. **b** *Wired-OR readout*: 3×3 array example. **c** *Unique-signal decoder*: only the channel(s) presenting a unique digitized voltage is recorded in the output. Examples of unique and non-unique activated locations at two time steps are also shown

is indicated by a uniquely decoded row and column (pulse at t = 1 in Fig. 24.12c). On the other hand, if multiple pulses from different channels occur at the same time step (i.e., the quantized voltages on many channels are equal) multiple rows and/or columns are activated, and no uniquely decoded channel is indicated (pulse at t = 5 in Fig. 24.12c). Only the uniquely decoded samples are stored, leading to substantial compression (output in Fig. 24.12c).

Direct measurements from large collections of RGCs indicate that this compression approach is effective for reconstructing real neural spikes. The probability distribution of the input signal reveals that spikes primarily inhabit the tails (Fig. 24.13a), which implies that voltages associated with spikes tend to be unique. Consequently, spike samples are typically retained while other samples are typically discarded (Fig. 24.13b). The result is an accurate reconstruction of spike waveforms (Fig. 24.13c) accompanied by substantial compression (~40x). Most importantly, these approximately reconstructed waveforms are sufficient to distinguish spikes

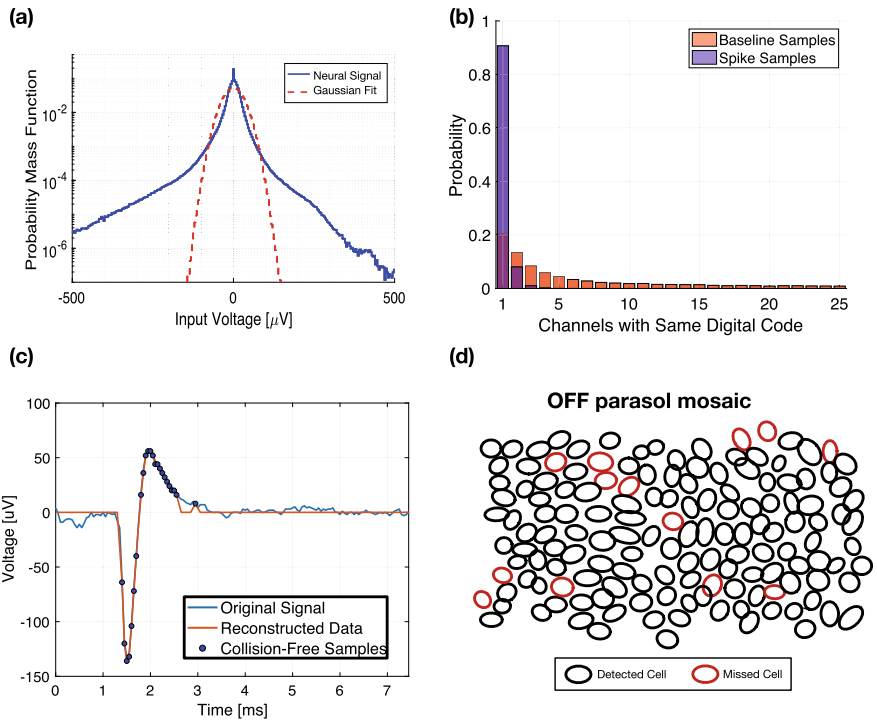

Fig. 24.13 Neural signal characteristics and compressive readout results. **a** Probability mass function of 100,000 samples from 512-electrode recording, after offset removal. **b** Probability of channels having the same digitized voltage for spike and baseline samples—here, baseline samples refer to samples that are within $\pm 4\sigma_n$ (standard deviation of noise in the recording channel) and spike samples refer to samples outside the $\pm 4\sigma_n$ band. Results from data recorded in isolated primate retina. **c**, **d** Example of a reconstructed spike (**c**) and a reconstructed OFF parasol mosaic (**d**) in the primate retina using the described readout strategy

from different cells, allowing recordings from nearly complete collections of neurons (~95%; Fig. 24.13d and [64]).

24.5.2 Dictionary Calibration

Dictionary calibration involves learning how current passed through the stimulating electrodes activates RGCs (Fig. 24.10b). The dictionary consists of elements that indicate the probability of generating a spike in each of the recorded RGCs, given a particular set of stimulating electrode(s) and current(s) [65]. Typically, for each dictionary entry, one or a few electrodes are used and a small number of cells are activated (but more complex dictionary entries are also possible). The generation of this dictionary is critical to obtain single-cell resolution. For each possible electrode and current level on that electrode, stimulation is applied, and the neural response is recorded on the entire array. The evoked response is compared against all the recorded EIs to identify which cell(s), if any, were activated (*response ID*). This step is performed repeatedly to estimate the probability of response of each RGC. The combined information about electrical stimulation and cellular activation probability constitutes one element in the dictionary. Note that dictionary elements which include axon bundle activation are typically not used (see Sect. 24.4 and [13]).

Challenges: A serious technical challenge for the above calibration is removing the *stimulation artifact* resulted from injecting a current into the high electrode impedance. Stimulation artifacts are large recorded waveforms that can obscure the neural response of interest, and are thus a severe problem for bi-directional neural interfaces. Typically, a combination of front-end mitigation techniques and back-end cancellation methods have to be implemented to overcome this issue [66]. Another challenge is the size of the dictionary: it is impractical to characterize the responses of all cells to all possible patterns of stimulation through a large electrode array. Approaches to this problem currently being explored include adaptive methods for developing models of electrically-evoked response [67], the use of prior information obtained from recording to predict the results of stimulation [67], and modeling interactions between electrodes in producing electrical stimulation [52].

24.5.3 Runtime

Runtime operation involves stimulating the available cells based on the incoming image, using the dictionary calibration (Fig. 24.10c). An external camera captures the visual scene, and the eye position is used to extract a focal image, i.e. the region of visual space that the interface should be encoding. Given the focal image, the goal is to optimize the stimulation pattern in real time such that the elicited cell responses lead to a faithful perception of the focal image (*dictionary approximation*). An obvious approach is to approximately mimic the normal RGC responses that

would be produced by the focal image, using existing understanding of natural image coding by the various RGC types, and the available dictionaryelements. A different approach is to assume a model for how the brain interprets the visual information transmitted by the retina, and tune the evoked RGC responses accordingly to optimize perception. These two approaches have benefits and drawbacks that depend on both the richness of the dictionary and the degree of our understanding of how the brain interprets visual signals. In either case, the calibrated dictionary is leveraged to efficiently determine the desired electrical activation of RGCs.

Challenges: In general, a large collection of RGCs must be activated to produce useful vision. This usually requires passing current through many electrodes. However, as described above, a dictionary that specifies RGC responses to all possible patterns of current through many electrodes would be prohibitively large to create and store on an implantable chip. To avoid this problem, temporal dithering of simpler (e.g. single-electrode) stimulation patterns has been proposed [65], with stimulation patterns from the dictionary interleaved at sub-millisecond time resolution—faster than the integration time of the brain. Results from ex vivo experiments show that greedily selecting the stimulation sequence from a simple dictionary to most rapidly reduce the expected error between the target image and a linear image reconstruction from the neural responses (as a surrogate for perception) leads to an efficient encoding of the image. However, future algorithms could improve upon the strong assumptions of this approach—such as integration times, independence of dictionary elements, linearity of perception, measures of perceptual error, the role of eye movements—while allowing for efficient runtime implementation in portable hardware.

24.5.4 System Architecture

To accomplish the above goals, we envision a system with a minimalist device implanted at the back of the eye that maximizes the number of channels within the tight power budget, while the more complex system components are implemented elsewhere (Fig. 24.14). The interface communicates wirelessly with a relay on the outside of the eye, which in turn communicates with a digital signal processing (DSP) chip outside the body. Finally, a camera and an eye tracker provide the desired image to the DSP. In this system, the data for calibration can be sent out to be processed by experts in the clinic, while the patient keeps using the device. During runtime operation, the DSP processes the data from the camera and the eye sensor and transmits the stimulation control signals appropriate for the focal image to the interface, via the relay.

Challenges: Novel circuits and systems are required to implement the bi-directional neural interface, the data-power relay, and the runtime DSP chip. The interface needs to maximize the number of channels, while maintaining low power, data bandwidth, and area for implantation. The implanted relay chip will optimize the wireless power and data link for efficiency, helping to overcome the difficulties introduced by eye

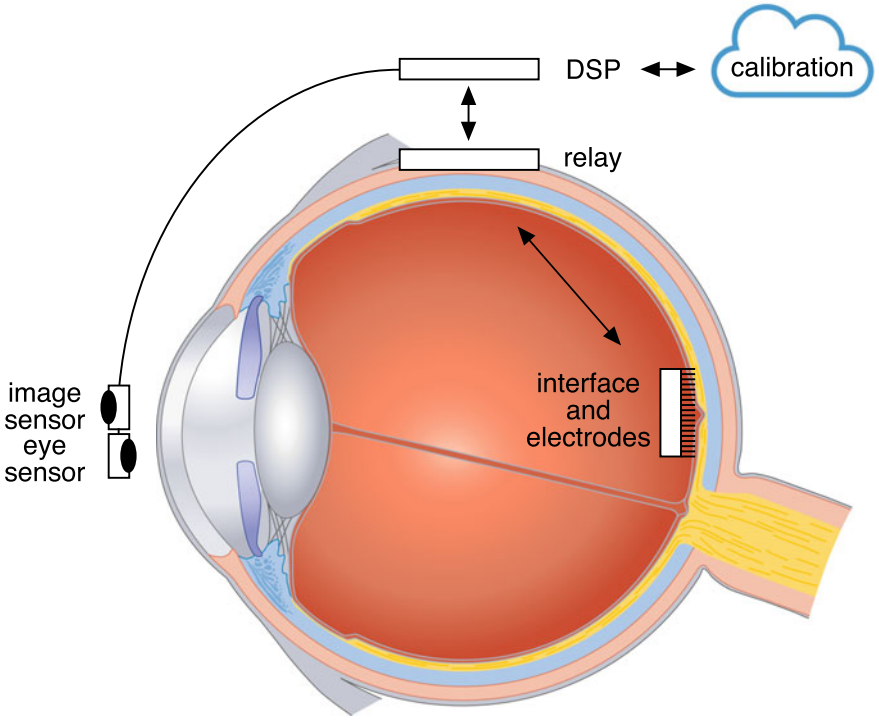

Fig. 24.14 Conceptual sketch of the Stanford Artificial Retina

movements and the different wireless communication environments inside and outside the eye. While the DSP chip will not be implanted and thus will have more power available, it will also have to implement compute-intensive algorithms that operate in real time with short latencies. Finally, other system challenges need to be faced, such as high precision eye movement tracking, encapsulation of active devices for long term implantation, CMOS-MEA integration, and surgical procedures. All these challenges will promote innovation in IC design and system integration.

24.6 Conclusion

Future retinal implants for restoring vision will need to achieve cell and cell-type resolution over a large area of the central retina to overcome the limitations of current devices. To do so requires novel circuits and systems coupled to bi-directional neural interfaces that interact efficiently with the neural circuitry via large and dense electrode arrays. The retina is an ideal target for pioneering this kind of high-fidelity, adaptive neuroengineering, as it is relatively accessible and well-understood. The Stanford

Artificial Retina is the first attempt at such an architecture, exploiting data-driven algorithm-circuit co-design for high-fidelity artificial vision.

In addition to treating incurable blindness, such a device may open other doors as well. Once the device is developed and able to interface specifically and configurably to many distinct RGC types, various scientific, medical, and commercial applications become possible. Scientifically, one may be able to modify the neural code of the retina in diverse ways to test how subtle and targeted alterations of the natural visual signal, such as changes in spike timing or cell type signaling diversity, influence visual acuity in experimental animals, and perhaps in humans that have already been implanted. Medically, it may be possible to encode visual scenes in abstracted or augmented ways in order to provide an artificial visual signal that is of even greater utility to the patient. Commercially, diverse applications of augmented artificial vision may also become possible, if implantation of the retina becomes safe and routine.

These technology developments may also have important implications for a wide range of BMIs. Many neural circuits in the brain share the essential architecture of the retinal circuitry: many cell types, intermixed, transmitting distinct signals to distinct targets for distinct functions. Thus, as our understanding of other areas of the nervous system increases, interfaces capable of reproducing the natural pattern of activation of neurons of different types may provide much higher performance in a range of BMI applications. The circuits and systems we propose for the artificial retina may be adaptable to future high-fidelity interfaces to the brain.

Acknowledgements The authors would like to thank Marty Breidenbach, Ruwan Silva, Stephen Weinreich, Matthias Kuhl, Daniel Palanker, Nishal Shah and the Stanford Artificial Retina Group [54] for useful discussions and comments, and Peter Li, Chris Sekirnjak, and Nora Brackbill for figure contributions. DM, EJC and the Stanford Artificial Retina Project are funded by the Wu Tsai Neurosciences Institute. EJC is funded by NEI grant EY021271 and a Stein Innovation Award from Research to Prevent Blindness.

References

1. M.W. Slutzky, Brain-machine interfaces: powerful tools for clinical treatment and neuroscientific investigations. Neuroscientist **25**, 139–154 (2019)
2. M.A. Lebedev, M.A.L. Nicolelis, Brain-machine interfaces: from basic science to neuroprostheses and neurorehabilitation. Physiol. Rev. **97**, 767–837 (2017)
3. A.H. Marblestone, B.M. Zamft, Y.G. Maguire, M.G. Shapiro, T.R. Cybulski, J.I. Glaser, D. Amodei, P.B. Stranges, R. Kalhor, D.A. Dalrymple, D. Seo, E. Alon, M.M. Maharbiz, J.M. Carmena, J.M. Rabaey, E.S. Boyden, G.M. Church, K.P. Kording, Physical principles for scalable neural recording. Front. Comput. Neurosci. **7**, 137 (2013)
4. G.W. Fraser, S.M. Chase, A. Whitford, A.B. Schwartz, Control of a brain–computer interface without spike sorting. J. Neural Eng. **6**, 055004 (2009)
5. C.A. Chestek, V. Gilja, P. Nuyujukian, J.D. Foster, J.M. Fan, M.T. Kaufman, M.M. Churchland, Z. Rivera-Alvidrez, J.P. Cunningham, S.I. Ryu, K.V. Shenoy, Long-term stability of neural prosthetic control signals from silicon cortical arrays in rhesus macaque motor cortex. J. Neural Eng. **8**, 045005 (2011)

6. B.P. Christie, D.M. Tat, Z.T. Irwin, V. Gilja, P. Nuyujukian, J.D. Foster, S.I. Ryu, K.V. Shenoy, D.E. Thompson, C.A. Chestek, Comparison of spike sorting and thresholding of voltage waveforms for intracortical brain-machine interface performance. J. Neural Eng. **12**, 016009 (2015)
7. J. Li, Z. Li, Sums of spike waveform features for motor decoding. Front. Neurosci. **11**, 406 (2017)
8. E.M. Trautmann, S.D. Stavisky, S. Lahiri, K.C. Ames, M.T. Kaufman, D.J. O'Shea, S. Vyas, X. Sun, S.I. Ryu, S. Ganguli, K.V. Shenoy, Accurate estimation of neural population dynamics without spike sorting. Neuron **103**, 292–308.e4 (2019)
9. N. Even-Chen, D.G. Muratore, S.D. Stavisky, L.R. Hochberg, J.M. Henderson, B. Murmann, K.V. Shenoy, Motor intracortical interface design opportunities for an order of magnitude power saving. Nat. Biomed. Eng. (2020) (In Press)
10. G.A. Goetz, D.V. Palanker, Electronic approaches to restoration of sight. Rep. Prog. Phys. **79**, 096701 (2016)
11. E.R. Kandel, J.H. Schwartz, T.M. Jessell, *Principles of Neural Science* (McGraw-Hill, New York, 2012)
12. C.E. Schoonover, *Portraits of the Mind: Visualizing the Brain from Antiquity to the 21st Century*. Abrams (2010)
13. L.E. Grosberg, K. Ganesan, G.A. Goetz, S.S. Madugula, N. Bhaskhar, V. Fan, P. Li, P. Hottowy, W. Dabrowski, A. Sher, A.M. Litke, S. Mitra, E.J. Chichilnisky, Activation of ganglion cells and axon bundles using epiretinal electrical stimulation. J. Neurophysiol. **118**, 1457–1471 (2017)
14. A.L. Yarbus, *Eye Movements and Vision* (Plenum, New York, 1967)
15. R.W. Rodieck, *The First Steps in Seeing* (Sinauer, Sunderland, 1998)
16. B.A. Wandell, *Foundations of Vision* (Sinauer, Sunderland, 1995)
17. B. Roska, M. Meister, The retina dissects the visual scene into distinct features, in *The New Visual Neurosciences* (2014), pp. 163–182
18. T. Gollisch, M. Meister, Eye smarter than scientists believed: neural computations in circuits of the retina. Neuron **65**, 150–164 (2010)
19. M. Beyeler, A. Rokem, G.M. Boynton, I. Fine, Learning to see again: biological constraints on cortical plasticity and the implications for sight restoration technologies. J. Neural Eng. **14**, 051003 (2017)
20. P. Dayan, L.F. Abbott, *Theoretical Neuroscience: Computational and Mathematical Modeling of Neural Systems* (MIT Press, 2001)
21. H.G. Rey, C. Pedreira, R. Quian Quiroga, Past, present and future of spike sorting techniques. Brain Res. Bull. **119**, 106–117 (2015)
22. J.E. Chung, J.F. Magland, A.H. Barnett, V.M. Tolosa, A.C. Tooker, K.Y. Lee, K.G. Shah, S.H. Felix, L.M. Frank, L.F. Greengard, A fully automated approach to spike sorting. Neuron **95**, 1381–1394.e6 (2017)
23. D. Carlson, L. Carin, Continuing progress of spike sorting in the era of big data. Curr. Opin. Neurobiol. **55**, 90–96 (2019)
24. J.F. Fohlmeister, P.A. Coleman, R.F. Miller, Modeling the repetitive firing of retinal ganglion cells. Brain Res. **510**, 343–345 (1990)
25. D. Boinagrov, J. Loudin, D. Palanker, Strength-duration relationship for extracellular neural stimulation: numerical and analytical models. J. Neurophysiol. **104**, 2236–2248 (2010)
26. G.J. Chader, J. Weiland, M.S. Humayun, Artificial vision: needs, functioning, and testing of a retinal electronic prosthesis. Prog. Brain Res. **175**, 317–332 (2009)
27. E. Zrenner, Fighting blindness with microelectronics. Sci. Transl. Med. **5**, 210ps16 (2013)
28. A.T. Chuang, C.E. Margo, P.B. Greenberg, Retinal implants: a systematic review. Br. J. Ophthalmol. **98**, 852–856 (2014)
29. Y.H.-L. Luo, L. da Cruz, A review and update on the current status of retinal prostheses (bionic eye). Br. Med. Bull. **109**, 31–44 (2014)
30. K. Grifantini, Aiding the Eye, Watching the Brain: James Weiland, IEEE Fellow, explores the unique challenges of retinal prostheses. IEEE Pulse **8**, 39–41 (2017)

31. M.S. Humayun, E. de Juan, G. Dagnelie Jr., The bionic eye: a quarter century of retinal prosthesis research and development. Ophthalmology **123**, S89–S97 (2016)
32. D. Nanduri, M.S. Humayun, R.J. Greenberg, M.J. McMahon, J.D. Weiland, Retinal prosthesis phosphene shape analysis, in *2008 30th Annual International Conference of the IEEE Engineering in Medicine and Biology Society* (2008), pp. 1785–1788
33. C. de Balthasar, S. Patel, A. Roy, R. Freda, S. Greenwald, A. Horsager, M. Mahadevappa, D. Yanai, M.J. McMahon, M.S. Humayun, R.J. Greenberg, J.D. Weiland, I. Fine, Factors affecting perceptual thresholds in epiretinal prostheses. Invest. Ophthalmol. Vis. Sci. **49**, 2303–2314 (2008)
34. A. Caspi, J.D. Dorn, K.H. McClure, M.S. Humayun, R.J. Greenberg, M.J. McMahon, Feasibility study of a retinal prosthesis: spatial vision with a 16-electrode implant. Arch. Ophthalmol. **127**, 398–401 (2009)
35. R.J. Jensen, J.F. Rizzo 3rd, O.R. Ziv, A. Grumet, J. Wyatt, Thresholds for activation of rabbit retinal ganglion cells with an ultrafine, extracellular microelectrode. Invest. Ophthalmol. Vis. Sci. **44**, 3533–3543 (2003)
36. A. Butterwick, A. Vankov, P. Huie, Y. Freyvert, D. Palanker, Tissue damage by pulsed electrical stimulation. IEEE Trans. Biomed. Eng. **54**, 2261–2267 (2007)
37. S.F. Cogan, Neural stimulation and recording electrodes. Annu. Rev. Biomed. Eng. **10**, 275–309 (2008)
38. D.R. Merrill, M. Bikson, J.G.R. Jefferys, Electrical stimulation of excitable tissue: design of efficacious and safe protocols. J. Neurosci. Methods **141**, 171–198 (2005)
39. L.S. Robblee, T.L. Rose, Electrochemical guidelines for selection of protocols and electrode materials for neural stimulation, in *Neural Prostheses: Fundamental Studies* (1990), pp. 25–66
40. A. Horsager, S.H. Greenwald, J.D. Weiland, M.S. Humayun, R.J. Greenberg, M.J. McMahon, G.M. Boynton, I. Fine, Predicting visual sensitivity in retinal prosthesis patients. Invest. Ophthalmol. Vis. Sci. **50**, 1483–1491 (2009)
41. J.-H. Jung, D. Aloni, Y. Yitzhaky, E. Peli, Active confocal imaging for visual prostheses. Vis. Res. **111**, 182–196 (2015)
42. E. Zrenner, K.U. Bartz-Schmidt, H. Benav, D. Besch, A. Bruckmann, V.-P. Gabel, F. Gekeler, U. Greppmaier, A. Harscher, S. Kibbel, J. Koch, A. Kusnyerik, T. Peters, K. Stingl, H. Sachs, A. Stett, P. Szurman, B. Wilhelm, R. Wilke, Subretinal electronic chips allow blind patients to read letters and combine them to words. Proc. R. Soc. B Biol. Sci. **278**, 1489–1497 (2011)
43. H. Lorach, G. Goetz, R. Smith, X. Lei, Y. Mandel, T. Kamins, K. Mathieson, P. Huie, J. Harris, A. Sher, D. Palanker, Photovoltaic restoration of sight with high visual acuity. Nat. Med. **21**, 476–482 (2015)
44. L.H. Jepson, P. Hottowy, G.A. Weiner, W. Dabrowski, A.M. Litke, E.J. Chichilnisky, High-fidelity reproduction of spatiotemporal visual signals for retinal prosthesis. Neuron **83**, 87–92 (2014)
45. C. Sekirnjak, P. Hottowy, A. Sher, W. Dabrowski, A.M. Litke, E.J. Chichilnisky, High-resolution electrical stimulation of primate retina for epiretinal implant design. J. Neurosci. **28**, 4446–4456 (2008)
46. L.H. Jepson, P. Hottowy, K. Mathieson, D.E. Gunning, W. Dabrowski, A.M. Litke, E.J. Chichilnisky, Focal electrical stimulation of major ganglion cell types in the primate retina for the design of visual prostheses. J. Neurosci. **33**, 7194–7205 (2013)
47. A.M. Litke, N. Bezayiff, E.J. Chichilnisky, W. Cunningham, W. Dabrowski, A.A. Grillo, M. Grivich, P. Grybos, P. Hottowy, S. Kachiguine, R.S. Kalmar, K. Mathieson, D. Petrusca, M. Rahman, A. Sher, What does the eye tell the brain?: Development of a system for the large-scale recording of retinal output activity. IEEE Trans. Nucl. Sci. **51**, 1434–1440 (2004)
48. E.J. Chichilnisky, R.S. Kalmar, Functional asymmetries in ON and OFF ganglion cells of primate retina. J. Neurosci. **22**, 2737–2747 (2002)
49. E.S. Frechette, A. Sher, M.I. Grivich, D. Petrusca, A.M. Litke, E.J. Chichilnisky, Fidelity of the ensemble code for visual motion in primate retina. J. Neurophysiol. **94**, 119–135 (2005)
50. G.D. Field, J.L. Gauthier, A. Sher, M. Greschner, T.A. Machado, L.H. Jepson, J. Shlens, D.E. Gunning, K. Mathieson, W. Dabrowski, L. Paninski, A.M. Litke, E.J. Chichilnisky, Functional connectivity in the retina at the resolution of photoreceptors. Nature **467**, 673–677 (2010)

51. V.H. Fan, L.E. Grosberg, S.S. Madugula, P. Hottowy, W. Dabrowski, A. Sher, A.M. Litke, E.J. Chichilnisky, Epiretinal stimulation with local returns enhances selectivity at cellular resolution. J. Neural Eng. **16**, 025001 (2019)
52. L.H. Jepson, P. Hottowy, K. Mathieson, D.E. Gunning, W. Dąbrowski, A.M. Litke, E.J. Chichilnisky, Spatially patterned electrical stimulation to enhance resolution of retinal prostheses. J. Neurosci. **34**, 4871–4881 (2014)
53. C.E. Rhoades, N.P. Shah, M.B. Manookin, N. Brackbill, A. Kling, G. Goetz, A. Sher, A.M. Litke, E.J. Chichilnisky, Unusual physiological properties of smooth monostratified ganglion cell types in primate retina. Neuron **103**, 658–672.e6 (2019)
54. Stanford Artificial Retina Project. http://med.stanford.edu/artificial-retina.html
55. E. Richard, G.A. Goetz, E.J. Chichilnisky, Recognizing retinal ganglion cells in the dark, in *Advances in Neural Information Processing Systems* (2015), pp. 2476–2484
56. V. Karkare, S. Gibson, D. Marković, A 75-μW, 16-channel neural spike-sorting processor with unsupervised clustering. IEEE J. Solid-State Circuits **48**, 2230–2238 (2013)
57. M. Pagin, M. Ortmanns, A neural data lossless compression scheme based on spatial and temporal prediction, in *2017 IEEE Biomedical Circuits and Systems Conference (BioCAS)* (2017), pp. 1–4
58. C. Aprile, K. Ture, L. Baldassarre, M. Shoaran, G. Yilmaz, F. Maloberti, C. Dehollain, Y. Leblebici, V. Cevher, Adaptive learning-based compressive sampling for low-power wireless implants. IEEE Trans. Circuits Syst. I Regul. Pap. **65**, 3929–3941 (2018)
59. T. Wu, W. Zhao, E. Keefer, Z. Yang, Deep compressive autoencoder for action potential compression in large-scale neural recording. J. Neural Eng. **15**, 066019 (2018)
60. T. Okazawa, I. Akita, A time-domain analog spatial compressed sensing encoder for multi-channel neural recording. Sensors **18**, 184 (2018). https://doi.org/10.3390/s18010184
61. V. Majidzadeh, A. Schmid, Y. Leblebici, A 16-channel, 359 μW, parallel neural recording system using Walsh-Hadamard coding, in *Proceedings of the IEEE 2013 Custom Integrated Circuits Conference* (2013), pp. 1–4
62. D. Tsai, R. Yuste, K.L. Shepard, Statistically reconstructed multiplexing for very dense, high-channel-count acquisition systems. IEEE Trans. Biomed. Circuits Syst. **12**, 13–23 (2018)
63. M. Sharma, A.T. Gardner, H.J. Strathman, D.J. Warren, J. Silver, R.M. Walker, Acquisition of neural action potentials using rapid multiplexing directly at the electrodes. Micromachines (2018). https://doi.org/10.3390/mi9100477
64. D.G. Muratore, P. Tandon, M. Wootters, E.J. Chichilnisky, S. Mitra, B. Murmann, A data-compressive wired-or readout for massively parallel neural recording. IEEE Trans. Biomed. Circuits Syst. **13**, 1128–1140 (2019)
65. N.P. Shah, S. Madugula, L. Grosberg, G. Mena, P. Tandon, P. Hottowy, A. Sher, A. Litke, S. Mitra, E.J. Chichilnisky, Optimization of electrical stimulation for a high-fidelity artificial retina, in *2019 9th International IEEE/EMBS Conference on Neural Engineering (NER)* (2019)
66. A. Zhou, B.C. Johnson, R. Muller, Toward true closed-loop neuromodulation: artifact-free recording during stimulation. Curr. Opin. Neurobiol. **50**, 119–127 (2018)
67. N.P. Shah, S. Madugula, P. Hottowy, A. Sher, A. Litke, L. Paninski, E.J. Chichilnisky, Efficient characterization of electrically evoked responses for neural interfaces, in *Neural Information Processing Systems (NeurIPS)* (2019)